60-year drought analysis of meteorological data in the western Po river Basin

Emanuele Mombrini[1], Stefania Tamea[1], Alberto Viglione[1], and Roberto Revelli[1,†]

[1]Dipartimento di Ingegneria dell'Ambiente, del Territorio e delle Infrastrutture (DIATI), Politecnico di Torino, Torino.
[†]deceased, 6 May 2023

Correspondence: Emanuele Mombrini (emanuele.mombrini@polito.it)

Abstract. Since the start of the 21st century, increasing focus has been put on drought and its wide range of environmental and socioeconomic effects, particularly in the context of climate change. The detection of drought changes has been done at different spatiotemporal scales and using different approaches with results that may not be fully comparable. This study aims to analyze drought trends in the northwestern region of Italy, encompassing the Piedmont and Aosta Valley regions, characterized by diverse topography and warming rates. The analysis is carried out over the last 60 years using the Standardized Precipitation Index (SPI) and Standardized Precipitation Evapotranspiration Index (SPEI) at 3- and 12-month timescales and deriving drought events at the local and regional spatial scales. By leveraging on a continuous and spatially coherent precipitation and temperature dataset, we explore the temporal and spatial variability of drought conditions and compare and contrust results obtained with different approaches.

Our results reveal widespread drying trends in the region, with temperature playing a crucial role. SPEI indicates more extensive and steeper negative trends than SPI due to temperature increases. However, the onset and cessation of drought events are predominantly driven by precipitation anomalies, while temperature plays a key role in longer-term drought conditions. Both SPI and SPEI indices identify consistently local and regional drought periods. In the 1990-2020 period, drought severity, duration, and intensity have generally increased compared to the 1960-1990 period, even though the change is less significant that the one obtained by analysing the indices themselves. Interestingly, the spatial scale of the analysis plays a significant role in interpreting these trends. Local drought characteristics are more influenced by temperature increases in SPEI, whereas regional droughts are more affected by precipitation patterns, as seen in SPI, with more frequent short-term droughts aggregating into longer-term deficits. Drying trends are more pronounced in lower, less rugged areas, while alpine regions show fewer drought trends. Interestingly, drought characteristics and trends are found to be more correlated to terrain ruggedness than to mean elevation. Significantly, a clear drying trend is not found at a region-wide level but is instead found when considering homogeneous areas defined by terrain ruggedness. Furthermore, changes in the number of drought episodes and in their severity, duration and intensity are found to be correlated with terrain ruggedness at all time scales.

These findings emphasize the need for high-resolution, region-specific studies to better understand how droughts evolve in complex terrains like the northwestern Italian Alps. Future research should investigate whether similar outcomes are found in other regions and what are the potential causes. Together with this study, this is instrumental to evaluate how these trends may continue to evolve under projected climate change scenarios.

1 Introduction

Drought is considered to be one of the main natural disasters, with widespread effects affecting large portions of the world's population (Wallemacq et al., 2015) and causing severe financial losses (García-León et al., 2021) and ecosystem impacts (Crausbay et al., 2020). Drought also has both short- and long-term effects on water availability (IDMP, 2022), which are relevant when considering the global increase in water demand in the past and the predicted challenges in meeting that demand in the future (Unesco, 2018; Wada et al., 2016; Burek et al., 2016). These drought-related phenomena are also likely to become more impacting, as droughts are predicted to become more severe and frequent under climate change conditions (Dai, 2011, 2013; Trenberth et al., 2014; Ward et al., 2020; Pörtner et al., 2022). Understanding if and how changes will occur on a local scale is thus necessary in order to develop adequate adaptation responses.

Several studies on meteorological drought trends exist at the global and continental scales (e.g., Ault, 2020; Sergio M. Vicente-Serrano, 2022; Brian Ayugi, 2022). Many studies have also been carried out in Northern Italy –often in the context of the wider Mediterranean or alpine region– analyzing either precipitation series (Bordi and Sutera, 2002; Brunetti et al., 2002; Hoerling et al., 2012; Haslinger and Blöschl, 2017; Pavan et al., 2019) or precipitation and temperature series (Hanel et al., 2018; Falzoi et al., 2019; Arpa Piemonte and Regione Piemonte, 2020; Baronetti et al., 2020; Vogel et al., 2021). Overall, these studies have found an increase in meteorological drought occurrence in North-West Italy, particularly after the 1970s, even in the cases in which recent drought events have not been found to be exceptional if compared to historical records (Haslinger and Blöschl, 2017; Hanel et al., 2018). Despite some agreement about the changes in precipitation, the seasonality reported by the studies differs significantly, with precipitation decrease found either in the winter (Brunetti et al., 2002; Hoerling et al., 2012) or summer season (Haslinger et al., 2012; Hanel et al., 2018; Pavan et al., 2019). Among these studies, those also considering temperature values consistently showed rising temperatures, and thus a rise in evaporative demand, to be a main factor in drought increase.

Besides drought trends in wider areas, interest in regional expressions of climate change has also been growing. One of the most investigated regional phenomena is the enhancement of warming rates with elevation, or elevation-dependent warming, explored both on the basis of surface measurement (Mountain Research Initiative EDW Working Group, 2015, e.g.,) and of climate models (e.g., Palazzi et al., 2019). In general, despite conflicting results regarding the presence of an elevation effect on warming rates and the lack of adequate climate data for mountainous regions, a consensus on enhanced warming rates at higher altitudes emerges (Rangwala and Miller, 2012; Pepin et al., 2022). The change of orographic precipitation gradients, i.e. the elevation-dependent precipitation change, have also been widely investigated, with less consensus on the results. A comprehensive meta-analysis of both in-situ studies of precipitation data from mountainous regions (including the Alps) and of global gridded databases from the early 1950s to the late 2010s reported a relative decrease in precipitation compared to lowlands, although without high confidence (Pepin et al., 2022). Furthermore, analyses such as Giorgi et al. (2016) have shown the importance of the spatial resolution in understanding processes in topographically complex regions, reporting that increases in summer precipitation in higher elevation areas of the Alpine range could only be detected by dense observation networks and described by high-resolution regional climate models.

Several studies on meteorological droughts are based on evaluating drought indices, such as SPI (Standardized Precipitation Index) and SPEI (Standardized Precipitation Evapotranspiration Index), giving a statistical interpretation of the temporal variability of meteorological data. Besides the temporal variability of wetting/drying events, droughts are further characterized by the duration and intensity of these events, which are relevant and independent indicators of drought characteristics. Less investigated is the spatial variability in drought characteristics and the change in indices obtained by averaging over different areas (Haslinger et al., 2012) and possibly leading to different outcomes in terms of drought magnitude and trends. The spatial dimension is relevant not only when larger or smaller regions experience the adverse effects of droughts but also when droughts occur on complex terrains, ranging from lowlands, to hills and mountains. In this case, drought characteristics may differ among terrains and drought impacts may be diversified. Elevation is thus a main factor to be considered to describe this complexity but may not be the only one.

Given these considerations, in this study, we aim to tackle the following research questions:

1. Are there temporal trends in drought indices such as SPI and SPEI, and how do these trends translate into changes in the characteristics of drought events, in terms of duration, severity, and intensity?

2. Is there a relationship between drought trends and topographical characteristics of the landscape? And if so, is elevation the topographical variable most correlated to these trends?

3. Do these conclusions change if drought events are defined at different spatial scales?

To investigate these questions, an area such as the western Po river basin is particularly fit. The region is part of the European Alps that divides the Mediterranean and Continental Europe, with opposite projected changes in precipitation and different responses to climate oscillations. Also, the region comprises both wide plains, hilly areas, and high mountains, with possible effects of elevation gradients and topography on drought characteristics and trends. Despite the presence, as detailed above, of studies on drought in the chosen region, these lacked either the needed spatial resolution or the focus on different choices for drought characterization and on possible effects of terrain characteristics on drought conditions. A gridded data set of precipitation and temperature values obtained from gauging stations distributed at different elevations throughout the domain and spanning more than 60 years is analyzed by calculating the SPI and SPEI at a 3 month and 12 month time scale. The index series are analyzed in order to find trends in drought conditions, as well as changes in drought event characteristics (duration, severity, intensity) both at point and areal scale. Sections 2.1 and 3 describe the study area, the meteorological dataset and further data, and the analysis methods, including the SPI and SPEI indices. In Section 4 the results obtained from each analysis are reported, while in Section 5 the general conclusion derived from the study are discussed.

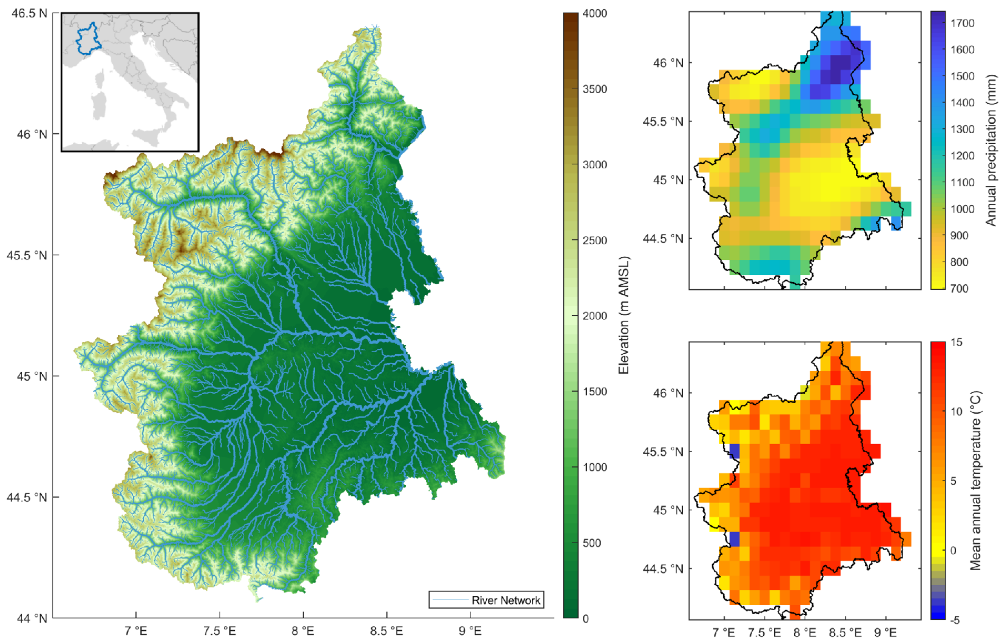

Figure 1. Map of the study area, including elevation, river network, mean annual precipitation and mean temperature values.

2 Data

2.1 Study area

The considered area includes the Piedmont region and the Aosta valley (Figure 1), located in the north-west of Italy, measuring more than 28000 km^2 and together representing the head of the Po river basin. Orographically, it is mainly a mountainous area surrounded by the Alpine chain, with mountain reliefs occupying half of the area and with the highest peaks lying in the Aosta Valley, while the plains lie in the central and eastern part of the region.

The area's reliefs play a key role in defining the area's climate variability (Arpa Piemonte, 2007): continental air masses from the Po plain, moist currents from the Mediterranean sea and north-western Atlantic currents interact with the reliefs leading to a complex and spatially variable climate (Ciccarelli et al., 2008). Annual precipitation ranges from 700 to more than 1700 mm, with a mean of 1000 mm. Annual precipitation is lowest in the central-west area and in north-western Aosta Valley, while highest in the norther area (Figure 1). Seasonality in precipitations is bimodal, with maxima in spring and autumn, and minima in summer and winter. For most of the region (close to 90%) winter is the season with minimum precipitation, and only in the south-west area the minimum is in summer; for the western and southern side of the territory (close to 60% of the overall area) the maximum precipitations occur in autumn, while for the central-eastern part they occur in spring (Perosino and Zaccara, 2006). Mean annual temperatures range from slightly over 13°C near the eastern border to slightly under -3.6°C at highest altitudes, closely following the altitude of the area.

2.2 Meteorological data source and processing

The data used in the analysis is obtained from the North Western Italy Optimal Interpolation (NWIOI) data set (Arpa Piemonte, Dipartimento Sistemi Provisionali, 2011), calculated and published by the Forecast Systems Department of the Regional Environmental Protection Agency of Piedmont (*Dipartimento Sistemi Previsionali - Arpa Piemonte*). The data set contains daily precipitation, and maximum and minimum temperature values over a regular grid covering the domain area with a 0.125° resolution. The data was obtained through an analysis of the region's meteorological station network data via the Optimal Interpolation method, as detailed in Uboldi et al. (2008).

The method spatially interpolates station data by correcting a previously defined background field based on an "area of influence" for each station. This area of influence is both horizontal and vertical in the case of temperature stations (tri-dimensional interpolation) and only horizontal in the case of precipitation stations (two-dimensional interpolation). In any case, no direct trend relation between the meteorological values and elevation has been evaluated and removed/added from the data. The data used in the interpolation method is provided by a gauging network covering both low and high-altitude areas, with changing availability of the number of available stations in time. Precipitation stations were about 120 till the mid 80s and have raised to the current 386 sites. Temperature stations were only about 25 in the first period and have then raised to 371. This is why the background field based on ERA40 has been used (see https://www.arpa.piemonte.it/scheda-informativa/spazializzazione-dei-dati-temperatura-precipitazione-griglia). Even though the change of number of stations in time, and therefore of information, may have an effect on the analyses described below, especially regarding local extreme drought situations, we believe that the advantage of having a long-term (1950s-2020s) and spatially consistent database is superior to the disadvantages due to its potential lack of homogeneity. The NWIOI grid is based on information from a much higher number of stations than other available datasets for the area (Turco et al., 2013) and it is therefore the most accurate and homogeneous data product of meteorological variables for the region. For the purpose of the subsequent analysis, 227 (the number of grid points inside the domain) series of 783 monthly values (December 1957 - February 2023) of precipitation, maximum and minimum temperature are calculated.

2.3 Land classification based on elevation

In order to study drought indices in relation to terrain characteristics, elevation values for the studied domain are used from the EarthEnv-DEM90 digital elevation model (Robinson et al., 2014) with 90 m resolution. Two sets of values are then obtained for each grid cell: the mean elevation (average of the elevation values inside a cell) and the terrain ruggedness. The terrain ruggedness (also known as surface roughness or topographic heterogeneity) is defined as the "deviations in the direction of the normal vector of a real surface from its ideal or intended form" (Whitehouse, 1994) and quantifies the irregularity of terrain; similarly to other studies, it is here calculated as the standard deviation of the elevation values inside every grid cell (Habib, 2021).

The landscape is classified in areas with similar topography. Four distinct areas of an almost equal number of cells are identified based on terrain ruggedness, which represent the plains, the hilly region, and the lower and higher mountains respectively.

Figure A1 shows the classified areas and the fact that mean elevation and terrain ruggedness are highly correlated. However, the advantage of using terrain ruggedness over mean elevation is that, in our study area, the hills in the center-south of the region are distinguished from the eastern flat part of the region, despite having similar mean elevation. Regardless of its simplicity, our terrain ruggedness classification is consistent with what one would obtain with the K3 Mountain classification (Karagulle et al., 2017), a much more complex categorization based on the Global Mountain Explorer 2.0 platform (Sayre et al., 2018).

3 Methods

This Section presents the methods adopted to tackle the three research questions stated in the introduction of the paper. The two drought indices, SPI and SPEI, are introduced in Sections 3.1 and 3.2. Then, we explain the methods used for assessing their trend in time (Section 3.3), for deriving drought events at the local and regional scale (Sections 3.4 and 3.5), and for assessing temporal changes of drought characteristics (Section 3.6). Explanation of the methods to analyze the relationship to terrain characteristics (mean elevation and local terrain ruggedness) is given in Sections 3.3, 3.4 and 3.6.

3.1 Standardized Precipitation Index (SPI)

Monthly precipitation values are used to calculate the Standardized Precipitation Index (McKee et al., 1993) at 3 and 12 month scale. The probability distribution chosen for the index calculation is the gamma distribution because, although other possible distributions have been proposed in the literature (Angelidis et al., 2012), including empirical ones (Laimighofer and Laaha, 2022), no single one was shown to be markedly better than the gamma distribution. Following the standard procedure found in the literature (Tigkas et al., 2015; Angelidis et al., 2012; Bordi and Sutera, 2002; Hayes et al., 1999), the index is thus obtained by fitting the gamma probability distribution $f(x) = \frac{1}{\Gamma(a)b^2} x^{a-1} e^{-x/b}$ to each month-of-the-year's series of values. To do this, the shape parameter a and the scale parameter b of the gamma distribution are calculated for each series of non-zero values of each month using the maximum likelihood method (Choi and Wette, 1969). The cumulative probability F_X is calculated as:

$$F_X(x_{i,j}) = \int_0^{x_{i,j}} f(x_{i,j})\,dx = \frac{1}{b_j^{a_j}\Gamma(a_j)} \int_0^{x_{i,j}} x_{i,j}^{a_j-1} e^{-x_{i,j}/b_j}\,dx \quad (1)$$

where j is the month index ($j = 1,2...12$), i is the year index ($i = 1,2...n$, with n years of records), and $\Gamma(a_j)$ is the gamma function, i.e. $\int_0^\infty y^{a_j-1} e^{-y}\,dy$.

To take the probability of zero values into account (given that the gamma distribution is defined for $x \in (0,\infty)$), the zero-inflated model is defined as:

$$H_X(x_{i,j}) = q_j + (1-q_j)F_X(x_{i,j}) \quad (2)$$

where q_j is the probability of zero precipitation for the j-th month of the year. Finally, the SPI is calculated as the normal inverse function of H_X via the formula:

$$SPI(x_{i,j}) = -\sqrt{2}\Phi^{-1}(H_X(x_{i,j})) \quad (3)$$

where Φ^{-1} is the inverse of the complementary error function:

$$\Phi(x) = \frac{2}{\sqrt{\pi}} \int_{x}^{\infty} e^{-t^2}\, dt \tag{4}$$

The SPI obtained through this method is thus a series of positive and negative values belonging to a normal distribution ($\mu = 0$, $\sigma = 1$): negative (positive) values represent precipitation below (above) the mean, with values lower than -1 denoting drought conditions (World Meteorological Organization, 2012). To calculate the index at a different time scale, a moving average is first applied to each monthly value, with length equal to the desired time scale and only previous data included; data that doesn't have enough preceding values to calculate the moving average is discarded. After calculating SPI on this data, each monthly value of the index describes how the conditions for a period with length equal to the time scale and ending in one particular month compare with all others in the series. For example, the SPI at 3-month time scale (SPI-3) for the month of July of a particular year indicates how much dry/wet the the previous 3 months have been compared with all other May-July periods in the series. In-built Matlab® functions are used for both the incomplete gamma function and its scale and shape parameters calculation and the calculation of the normal inverse function.

3.2 Standardized Precipitation Evapotranspiration Index (SPEI)

In order to take into account the effect of evaporative demand on drought episodes, and for comparison with SPI values, the Standardized Precipitation Evapotranspiration Index (Vicente-Serrano et al., 2010) is calculated at 3 and 12-month scale. The procedure for calculating the index is the same as the SPI, but the data analyzed is a series of monthly precipitation minus reference evapotranspiration (ET_0, in mm) values and a log-logistic probability distribution is used. Temperature data was used to calculate monthly ET_0 values using the Hargreaves formula (Hargreaves and Samani, 1985), following the recommendations for SPEI calculation (Beguería et al., 2014). Probability Weighted Moments (PWMs) using Hosking's unbiased method (Hosking, 1986) were used to calculate the α, β and γ parameters of the log-normal distribution for each month of the year, according to the formulae (again according to the recommendations for the index calculations found in Beguería et al., 2014):

$$w_{s_j} = \frac{1}{N} \sum_{i=1}^{N} \frac{\binom{N-i}{s} d_{i,j}}{\binom{N-1}{s}} \tag{5}$$

$$\beta_j = \frac{2w_{1_j} - w_{0_j}}{6w_{1_j} - w_{0_j} - 6w_{2_j}} \tag{6}$$

$$\alpha_j = \frac{(w_{0_j} - 2w_{1_j})\beta_j}{\Gamma(1+1/\beta_j)\Gamma(1-1/\beta_j)} \tag{7}$$

$$\gamma_j = w_{0_j} - \alpha_j \Gamma(1+1/\beta_j)\Gamma(1-1/\beta_j) \tag{8}$$

where $d_{i,j}$ are the precipitation minus ET_0 values for a given month j of the year i and w_{s_j} are the s order of the PWM for the month j. Using the α_j, β_j and γ_j parameters the log-logistic distribution is calculated as:

$$F_D(d_{i,j}) = \left[1 + \left(\frac{\alpha_j}{d_{i,j} - \gamma_j}\right)^{\beta_j}\right]^{-1} \tag{9}$$

Finally, this F_D distribution is transformed into a normal distribution to obtain the SPEI values. Again, moving average windows are applied to the input data in order to obtain different time scales. The distribution was shown to be well suited to analyze the data, as calculations obtained a finite solution for all series.

3.3 Trend analysis

Drought index series are analyzed in order to search for significant (at 5% significance) trends. The trends are estimated using the Theil-Sen slope estimator (Theil, 1950; Sen, 1968), i.e., by calculating the median slope between the indices values for all possible month pairs. The significance test is performed through the Mann-Kendall test (Mann, 1945), which is a non-parametric (distribution-free) alternative to the linear regression slope test available in regression analysis. To improve the power of the test, deseasonalization and pre-whitening of the data are performed. Deseasonalization is performed by subtracting the mean of the detrended temperature series for each month using the Climate Data Toolbox (Greene et al., 2019). The autocorrelation of the series (given that a moving average is applied at 3 and 12 month time scale) is taken into account by also applying different pre-whitening methods before performing trend analysis. These method are the simple Pre-Whitening method (PW, Kulkarni and Storch, 1995), the Trend Free Pre-Whitening method (TFPW, Yue et al., 2002) and the Variance Corrected Trend Free Pre-Whitening method (VCTFPW, Wang et al., 2015). The different results are used to obtain one trend evaluation by applying the 3PW algorithm (Collaud Coen et al., 2020), which, for the purpose of this study, is as follows: (a) if the lag-1 autocorrelation of the data is significant (following a normal distribution at the two-sided 95% confidence interval), the PW and TFPW series are obtained from the original series; (b) the trend is considered significant if both processed series return significant trends using the Mann-Kendall test; and (c) the slope of the significant trend is given as the Sen's slope of the VCTFPW series. If the lag-1 autocorrelation of a series is found not to be significant, trend analysis is performed on the un-modified data.

In order to identify whether different trends in the drought indices occur in areas with different landscape characteristics, the classification of the research area in four classes is used, as described in Section 2.3.

3.4 Local drought analysis

Each SPI/SPEI series obtained for the cells of the data grid (Section 2) is analyzed pixel-by-pixel through a "run analysis", at both time scales, in order to identify *local drought events* and study local drought characteristics. Based on run theory (Yevjevich, 1967), a drought run is a series of consecutive months under a certain threshold (-1, corresponding to a moderately dry condition in the SPI classification). Adding onto this definition, in the present study, the negative values leading and following a period under the -1 threshold are here counted as part of the runs, in order to capture events where a deficit is

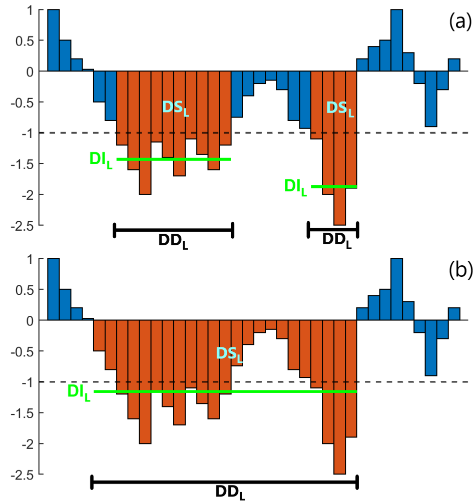

Figure 2. Drought runs examples, highlighted in orange. **(a)** Runs obtained with a simple -1 threshold (not used in this paper). **(b)** Run defined by a threshold and by including their onset and offset, i.e. all negative values before and after the values under the threshold (as used in this paper). In both cases $\mathrm{DS_L}$ is the sum of the index value during the run, $\mathrm{DD_L}$ is the length of each run and $\mathrm{DI_L}$ is the mean index value during the run.

not fully recovered from (see Figure 2). Drought run characteristics are then calculated for each local drought event (Caloiero et al., 2021):

- Drought Duration ($\mathrm{DD_L}$) is the length of the drought run, reported in months for this study;
- Drought Severity ($\mathrm{DS_L}$) is the cumulative value of the index during each run;
- Drought Intensity ($\mathrm{DI_L}$) is the ratio between the $\mathrm{DS_L}$ and $\mathrm{DD_L}$ value of a run, i.e. the average index value during the run.
- Drought maximum Intensity ($\mathrm{DmaxI_L}$) is the maximum (without sign) index value during the run.

Given a series of drought runs calculated from an index series, the average values of these characteristics for all runs are reported as $\overline{\mathrm{DD}}_\mathrm{L}$, $\overline{\mathrm{DS}}_\mathrm{L}$ and $\overline{\mathrm{DI}}_\mathrm{L}$. Pedex L indicates that these are *local* drought characteristics, as opposed to drought characteristics calculated over multiple grid points.

To quantify the level of correspondence between local droughts by SPI and SPEI, each cell's series is transformed into a binary series of zeros and ones, where 1 denotes the occurrence of a drought, and the Cohen's kappa (Cohen, 1960) between the series is calculated as a measure of agreement, with 0 and 1 denoting no agreement and complete agreement respectively.

In order to identify whether different trends in the drought indices occur in areas with different landscape characteristics, correlations between terrain characteristics and trend values are quantified by calculating both the Pearson and the Spearman correlation coefficients (Shevlyakov and Oja, 2016).

3.5 Region-wide drought event analysis

In order to include the spatial dimension in the study of droughts and to describe the coupled spatio-temporal characteristics of drought runs, the following approach is taken, similarly to González-Hidalgo et al. (2018), Baronetti et al. (2020) and Baronetti et al. (2022). In contrast to local droughts, which are calculated from a series of index values belonging to one cell, *region-wide drought events* are evaluated by considering what happens in the entire region. So, for example, during a region-wide drought event, a certain percentage of the domain will be in drought conditions (below the -1 drought index threshold); each of these cells will therefore be experiencing a local drought. Region-wide drought events are detected through the use of two thresholds: (1) an index threshold, based on the SPI/SPEI values (cells with an index lower than -1 are considered to be in drought condition); and (2) an area threshold (a drought episode is considered in progress when at least 25% of the domain is in drought condition). Note that the additional threshold on the minimum duration threshold of 3 weeks used in González-Hidalgo et al. (2018), Baronetti et al. (2020), and Baronetti et al. (2022) is always met as monthly data is used in this analysis. In addition to two thresholds listed above, the drought events' *onset* and *offset*, meaning the periods below the 25% drought area threshold before and after a period above the threshold, were also included in the drought event itself. This approach is useful in considering persisting drought conditions as one continuous event while still maintaining well-defined episodes, similar to the proposed local drought definition (see Figure 2).

Similarly to local drought, different characteristics are calculated for each region-wide drought event:

- Drought event Duration ($\mathrm{DD_E}$) is the length of the drought event;
- Drought event Severity ($\mathrm{DS_E}$) is the sum of the drought index of each cell in drought condition for the duration of the event, divided by the total number of cells in the domain;
- Drought event Intensity ($\mathrm{DI_E}$) is the mean of the local intensity for each cell that has been part of the drought event. Intensity for each cell is calculated as the sum of the drought index below the -1 threshold divided by the number of months where the index was lower than -1.
- Drought Area ($\mathrm{DA_E}$) is the average number of cells in drought condition during the event;

Given a series of region-wide drought events calculated from the index series for all cells in the domain, the average value of these characteristics for all events is reported as $\overline{\mathrm{DD}}_\mathrm{E}$, $\overline{\mathrm{DS}}_\mathrm{E}$, $\overline{\mathrm{DI}}_\mathrm{E}$ and $\overline{\mathrm{DA}}_\mathrm{E}$.

3.6 Change analysis of drought characteristics

In order to evaluate the significance of the change in average drought characteristics between the periods 1958-1990 and 1990-2023 (approximately the first and second half of the series), the two sample t-test (Rasch et al., 2011) is applied to $\overline{\mathrm{DS}}_\mathrm{L}$, $\overline{\mathrm{DD}}_\mathrm{L}$ and $\overline{\mathrm{DI}}_\mathrm{L}$ (as well as $\overline{\mathrm{DS}}_\mathrm{E}$, $\overline{\mathrm{DD}}_\mathrm{E}$, $\overline{\mathrm{DI}}_\mathrm{E}$ and $\overline{\mathrm{DA}}_\mathrm{E}$) calculated for the drought periods starting before and after January 1990, respectively. After obtaining the values pre and post 1990, their sample mean and standard deviations are calculated, and the test statistic t is calculated as

$$t = \frac{\overline{DC}_{post} - \overline{DC}_{pre}}{s} \tag{10}$$

where $\overline{DC}$ is the mean of a certain drought characteristics for all drought runs/events before/after 1990 and s:

$$s = \sqrt{\frac{\sigma^2_{post}}{n_{post}} + \frac{\sigma^2_{pre}}{n_{pre}}} \tag{11}$$

where σ is the standard deviation of a certain drought characteristics for all drought run/events before and after 1990 and n the number of run/events for the two periods. t is then compared with the critical value of the statistic at a 5% significance level. Given that no assumptions about the variance of the two ensembles were made, and given the different number of runs in the two periods, the degrees of freedom needed for the calculation of the critical value were approximated through the Welch-Satterthwaite equation (Welch, 1947).

Similarly to what is done for trends in drought indices, the correlation between changes in local drought characteristics and terrain characteristics (mean elevation and ruggedness) are quantified by the Pearson and the Spearman correlation coefficients (Shevlyakov and Oja, 2016).

4 Results

The following sections report the results of the analyses of drought indices (Section 4.1), local drought events (Section 4.2) and region-wide drought events (Section 4.3). For the first two analyses, the correlation of temporal trends with topographic characteristics of the landscape is reported in each section.

4.1 Trends in the drought indices

Drought indices, i.e. SPI and SPEI, calculated from the precipitation and temperature series of each cell in the region are analyzed in order to find possible trends in drought conditions. Given the nature of SPI, as described in Section 3.1, negative trends indicate a tendency for precipitation to be below the series's mean value. This means that both wet and dry periods have seen on average reduced precipitation, and thus that drought conditions, when occurring, have become worse. For the SPEI, described in Section 3.2, the trend interpretation is the same, but instead of precipitation a climatic water balance between precipitation and potential evapotranspiration is considered. Furthermore, trend analysis on indices at the shorter 3-month time scale and the longer 12-month time scale indicates, respectively, how drought conditions might have evolved over smaller time scales, closer to the response time of soil moisture conditions to meteorological conditions, and over larger time scales, closer to the response time of reservoirs and groundwater levels to meteorological conditions.

Trend analysis on SPI-3 and SPI-12 values shows a majority of cells with significant negative trends (and thus a tendency towards dryer conditions). A majority of cells (almost 70%) shows negative SPI trends at both 3 and 12-month time scale, although SPI-12 indicates dryer conditions over time compared to SPI-3 (Figure 3a-b). Trend analysis for SPEI-3 and SPEI-12

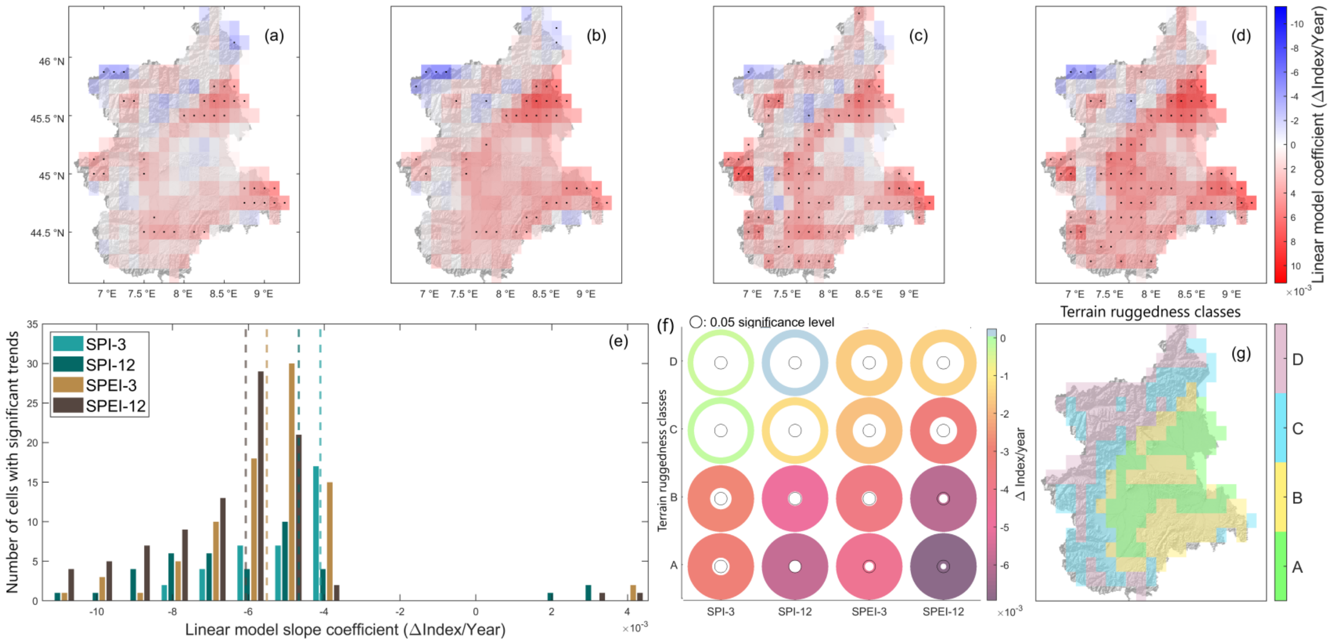

Figure 3. Trend analysis on drought indices. **(a)** SPI-3 trends. **(b)** SPEI-3 trends. **(c)** SPI-12 trends. **(d)** SPEI-12 trends. Cells containing a dot denote significant trends at 5% significance. **(e)** Frequency histogram of significant trends per distribution of trends' Sen-slope coefficients, with dashed lines representing the respective mean values of indexes. **(f)** Trend analysis on drought indices calculated from data belonging to areas defined by terrain ruggedness inside cells. The colour of the circles represents the slope coefficient of the trend, while the inner radius of the circles represents the significance of the trend (a smaller inner radius represents a more significant trend). The black circles denote a significance level of 5%. **(g)** Representation of terrain ruggedness classes (see Figure A1 for more details on their definition).

displays a similar time scale effect, with the longer time scale having a higher number of cells with significant trends (although with 79% of cells showing trends for both time scales) and, on average, greater slope coefficients (Figure 3c-d). The clearest differences emerge by comparing the results obtained by SPI and SPEI (Figure 3e). At both time scales, SPEI shows a far wider region heading towards dryer conditions (more than twice the cells found with SPI), and at a faster rate, given the slope coefficients.

From observing Panels a-d of Figure 3, clear and consistent spatial patterns are visible. The terrain characteristics align well, especially for the SPEI analysis. Even though terrain elevation is to be considered a potential variable correlated to trend patterns, an expert observer (or simply someone grown in the region) would spot the fact that the majority of the significant positive trends occur in flat areas, not necessarily the lower ones. Figures 3f-g show that, if terrain ruggedness is used to subdivide the area into regions with similar sizes, the low elevated areas (classes A and B), especially the flat ones (class A), show the strongest and most significant trends for both SPI and SPEI at both 3- and 12-month timescales. Classifying the area by terrain mean elevation (not shown here) gives similar results, i.e., a significant difference between the alpine range and the plain area of the domain with worsening drought conditions for the latter, but with smaller differences between the two classes with lower elevation.

4.2 Local drought analysis

After analyzing how the general drought conditions in the region have changed over time, the effects of such changes on the characteristics of local drought periods are investigated through a *run analysis* (see Section 3.4). First, the characteristics of local droughts in the region are described as a baseline; then, possible temporal changes in their number, severity, duration and intensity are investigated.

4.2.1 Local droughts characteristics

Despite the differences in observed trends detailed in the previous section, the detection of local droughts by SPI and SPEI shows a high level of correspondence for both 3 and 12-month time scales. The mean Cohen's kappa (Cohen, 1960) kappa value is slightly higher at the 3-month scale (mean kappa equal to 0.86) than at the 12-month scale (mean kappa equal to 0.81), but always higher than 0.5: this means that there is always good to excellent agreement between the identification of drought runs based on SPI and SPEI. Therefore, given that SPI drought runs are based only on precipitation values, it can be stated that a majority of local droughts are determined by precipitation deficits, with temperature itself having a smaller influence on single events, and a greater influence on overall trends (as seen in the comparison between drought indices trends reported in Section 4.1).

In the analysis of local drought characteristics (Figures 4), the longer time scale shows, both for SPI and SPEI, a lower number of runs, but with higher severity ($\mathrm{DS_L}$) and duration ($\mathrm{DD_L}$). Drought intensity ($\mathrm{DI_L}$) values are instead similar between the two time scales, although slightly greater at the 3-month scale. Despite the difference in absolute values, drought analysis indicates a higher number of local droughts, a higher $\overline{\mathrm{DS}}_\mathrm{L}$ and $\overline{\mathrm{DD}}_\mathrm{L}$ for SPEI runs compared to SPI runs at both time scales. Thus, when considering both precipitation and $\mathrm{ET_0}$, a greater number of longer and more severe drought periods are detected, compared to the less numerous and shorter periods detected using only precipitation.

One significant difference emerges when comparing the mean drought intensity ($\overline{\mathrm{DI}}_\mathrm{L}$) values. Average drought intensity is lower for SPEI-3 runs compared to SPI-3, while slightly greater for SPEI-12 compared to SPI-12. This seems to be due to the lower index values reported by SPI-3 compared with SPI-12. The mean negative minimum values during the drought runs are lower for SPI than for SPEI at both 3 months (-1.65 ± 0.05 for SPI and -1.47 ± 0.03 for SPEI) and 12 months (-1.52 ± 0.07 for SPI and -1.46 ± 0.06 for SPEI) time scales, but, while SPEI values remain almost constant, SPI values show less negative mean minimum values at the longer time scale. This fact, combined with the similarly longer SPEI droughts at both time scales leads to the slightly higher $\overline{\mathrm{DI}}_\mathrm{L}$ for SPEI-12.

Regarding the spatial distribution of mean local drought characteristics (number of runs, $\overline{\mathrm{DS}}_\mathrm{L}$, $\overline{\mathrm{DD}}_\mathrm{L}$ and $\overline{\mathrm{DI}}_\mathrm{L}$), SPI and SPEI show similar results when compared at the same time scale, while deviating significantly between 3 and 12-month time scales. SPI-3 and SPEI-3 drought characteristics do not display clear spatial gradients but do display some correlation with mean elevation and terrain ruggedness (Table 1, where only Pearson correlations are reported because Spearman correlations give

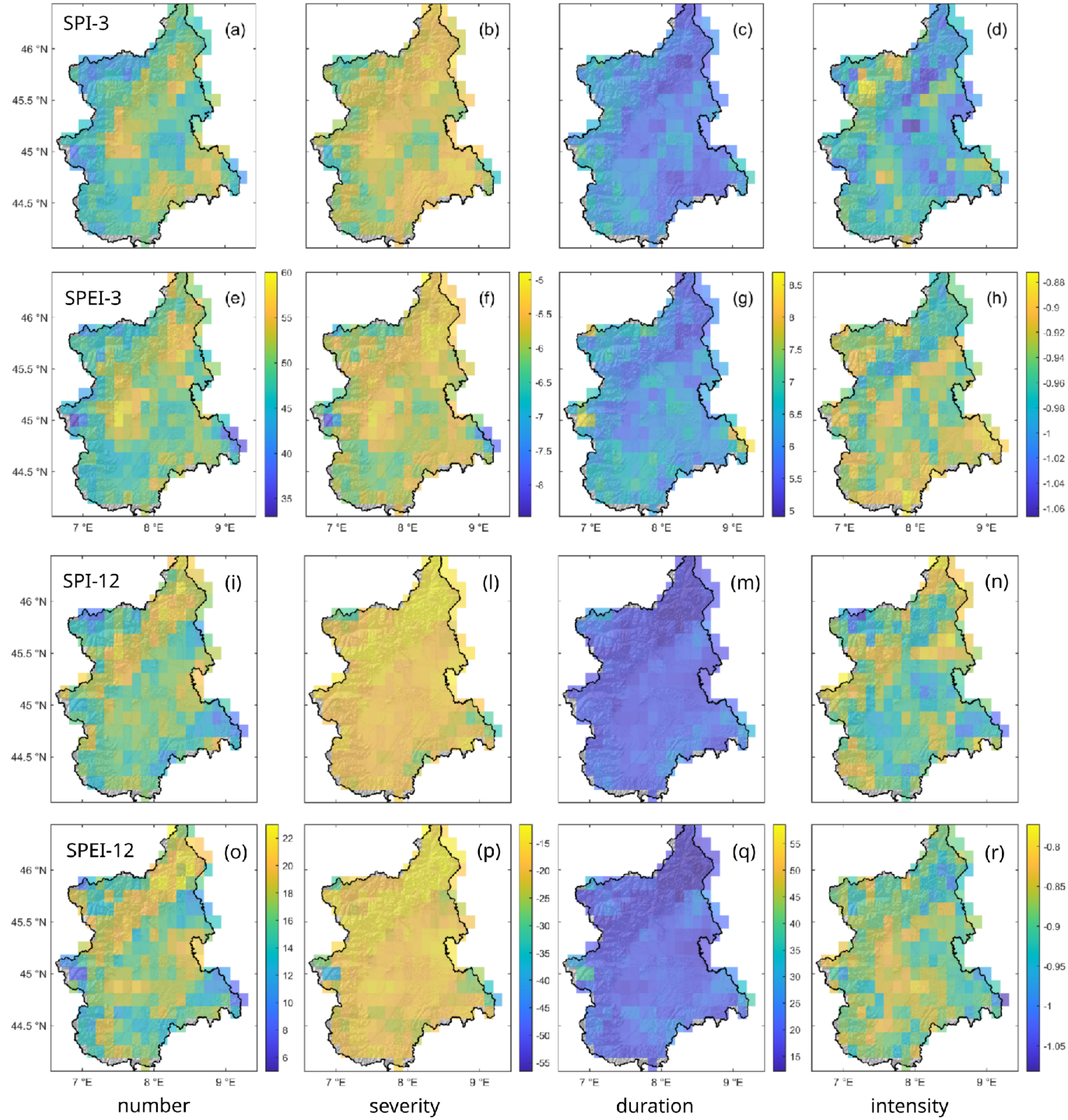

Figure 4. Spatial distribution of drought run characteristics at 3- and 12-month time scales. SPI-3's number of runs **(a)**, average severity of local drought $\overline{DS}_L$ **(b)**, average length of local drought $\overline{DD}_L$ **(c)**, average intensity of local drought $\overline{DI}_L$ **(d)**. SPEI-3's number of runs **(e)**, $\overline{DS}_L$ **(f)**, $\overline{DD}_L$ **(g)**, $\overline{DI}_L$ **(h)**. SPI-12's number of runs **(i)**, average severity of local drought $\overline{DS}_L$ **(l)**, average length of local drought $\overline{DD}_L$ **(m)**, average intensity of local drought $\overline{DI}_L$ **(n)**. SPEI-12's number of runs **(o)**, $\overline{DS}_L$ **(p)**, $\overline{DD}_L$ **(q)**, $\overline{DI}_L$ **(r)**.

Table 1. Pearson correlation coefficients between mean drought characteristics and mean elevation (EL) or terrain ruggedness (RG), for both SPI and SPEI at 3 an 12 month time scale. Values in italic font denote significant correlation at 5% significance.

	Number of runs		$\overline{DS}_L$		$\overline{DD}_L$		$\overline{DI}_L$	
	EL	RG	EL	RG	EL	RG	EL	RG
SPI-3	*-0.50*	*-0.40*	*-0.35*	*-0.22*	*0.44*	*0.29*	*0.28*	*0.21*
SPEI-3	*-0.29*	*-0.22*	*-0.15*	-0.06	*0.14*	0.02	-0.05	*-0.23*
SPI-12	0.06	*0.18*	0.13	*0.23*	-0.11	*-0.21*	*0.18*	*0.23*
SPEI-12	0.04	*0.19*	0.05	*0.19*	-0.07	*-0.21*	0.01	-0.03

very similar results). In particular, when areas at a higher mean elevation are considered, a lower number of more severe, longer and, for SPI-3 only, less intense droughts are reported (although with some differences in the degree of correlation). Altogether, these results indicate that, on shorter time scales, droughts in higher mean elevation areas tend to be more clustered. Even so, visual inspection of the spatial distribution of local drought characteristics for SPI-3 and SPEI-3 (see Figure 4a-h) shows that spatial variability of characteristics is overall quite high. Conversely, the higher mean elevation points of the mountainous part of the domain do show quite uniform drought characteristics consistent with the observed correlations. It can therefore be stated that, despite some significant effects of mean elevation on the characteristics of drought periods, local orography and meteorological conditions play a key role. When considering terrain ruggedness, the resulting correlation values are generally less significant than for mean elevation at the 3-month scale but more significant at the 12-month scale. SPI-12 and SPEI-12 run characteristics display no spatial gradient (see Figure 4i-r) and no correlation with mean elevation in terms of number, severity and duration of runs. The only statistically significant correlation found is with SPI-12's $\overline{DI}_L$, with higher mean elevation areas reporting less intense events, coherent with the results obtained for SPI-3. Conversely, indices at the 12 month scale have significant correlations with terrain ruggedness for the number of runs and their $\overline{DS}_L$ and $\overline{DD}_L$, with rugged terrain reporting less numerous, less severe and shorter droughts.

4.2.2 Temporal analysis of local drought characteristics

Trend analysis on the obtained local drought characteristics reports only a few cells (always less than 3% of the domain) showing significant changes for drought duration, severity and intensity (DD_L, DS_L and DI_L) (Figure 5). In comparison, SPEI-3 shows a far greater amount of cells, slightly more than 10% of the total area, with significant increasing trends for DS_L and DI_L, distributed almost exclusively along the alpine chain, particularly near the southern border. The yearly predicted change, in terms of percentage of the relative $\overline{DS}_L/\overline{DI}_L$ for the cell, ranges from 1 to 11% and 0.01 to 1% for severity and intensity respectively.

Despite the overall lack of significant trends, clear differences can be found between the characteristics of drought runs that started before and after 1990, approximately at half the series' length. SPI-3 and SPEI-3 display on average an increase in

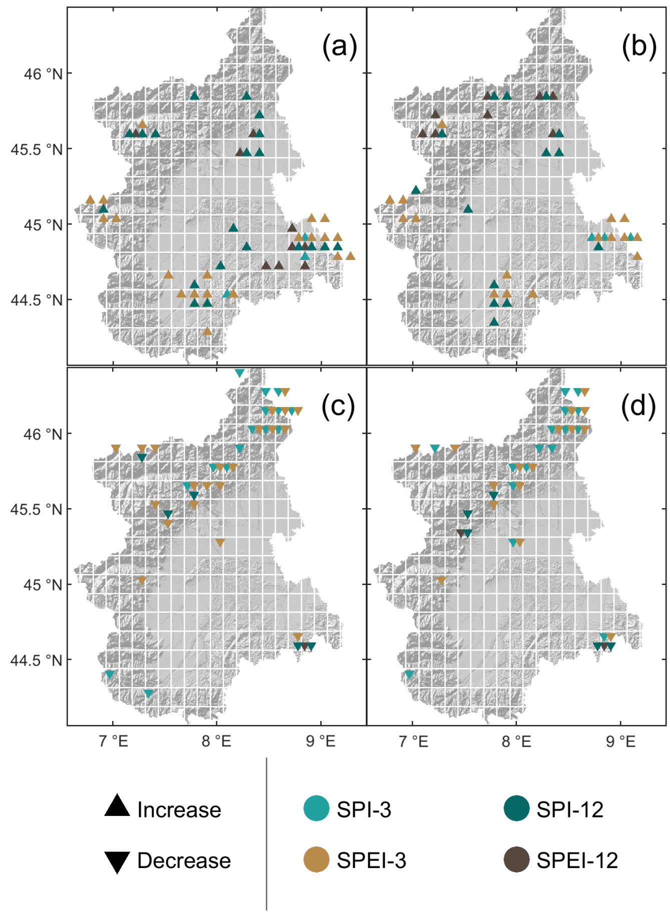

Figure 5. Cells with significant changes in mean drought characteristics between the 1958-1990 and 1990-2023 periods according to the two sample t-test. **(a)** Mean drought severity ($\overline{DS}_L$) increase, **(b)** Mean drought duration ($\overline{DD}_L$) increase, **(c)** Mean drought severity ($\overline{DS}_L$) decrease, **(d)** Mean drought duration ($\overline{DD}_L$) decrease.

the number of droughts (more markedly in the case of SPEI-3), and in their DI_L. Opposite results are found in terms of DS_L and DD_L, with SPI-3 indicating a shift towards less severe and shorter droughts, and vice-versa for SPEI-3. Significantly, this difference seems to be caused mainly by cells located in the flat part of the region, where SPEI-3 indicates a shift towards greater DS_L and DD_L (not shown here). The rest of the region shows similar results for the two indices. The alpine chain, especially in the north, shows a shift towards a higher number of less severe, shorter and less intense droughts. SPI-12 and SPEI-12, on the other hand, report agreeing results and show on average a change towards a lower number of more severe, longer and more intense droughts across the domain. The only exception is the alpine chain, where for a small but continuous area a change towards less numerous, less severe, shorter and less intense droughts is found.

These relative changes are highly correlated to the mean cell elevation and, even more so, to the ruggedness of the area (Table 2). Only Pearson correlations are reported in the table because Spearman correlations give very similar results. For

Table 2. Pearson correlation coefficients between change in mean drought characteristics pre- and post-1990 and mean elevation (EL) and terrain ruggedness (RG), for both SPI and SPEI at 3 an 12 month time scale. Values in italic font denote significant correlation at 5% significance.

	ΔNumber of runs		$\Delta\overline{\mathbf{DS}}_{\mathbf{L}}$		$\Delta\overline{\mathbf{DD}}_{\mathbf{L}}$		$\Delta\overline{\mathbf{DI}}_{\mathbf{L}}$	
	EL	RG	EL	RG	EL	RG	EL	RG
SPI-3	0.06	*0.18*	*0.29*	*0.42*	*-0.23*	*-0.37*	*0.36*	*0.41*
SPEI-3	*0.24*	*0.23*	*0.20*	*0.38*	*-0.21*	*-0.38*	0.13	*0.26*
SPI-12	*-0.28*	*-0.33*	*0.16*	*0.25*	*-0.19*	*-0.27*	0.04	0.09
SPEI-12	*-0.15*	*-0.25*	*0.16*	*0.32*	*-0.15*	*-0.30*	*0.15*	*0.28*

example, at the 3-month scale, the flat part of the region has seen a change towards less numerous, more severe, longer and more intense droughts, while the alpine chain shows an opposite change. Changes in SPEI-12 run characteristics also display a similar correlation for $\overline{\mathrm{DS}}_{\mathrm{L}}$, $\overline{\mathrm{DD}}_{\mathrm{L}}$ and $\overline{\mathrm{DI}}_{\mathrm{L}}$ but opposite in terms of number of droughts. Therefore, it seems that SPEI-12 droughts got more numerous, more severe, longer and more intense in the lowlands, and, although not quite as strongly, the opposite has happened in the alpine chain. SPI-12 does show an increase in the number, severity and duration of droughts in the lowlands and a decrease in the mountains, but no correlation for $\overline{\mathrm{DI}}_{\mathrm{L}}$.

Changes in local drought characteristics, as opposed to average values, report higher correlation with terrain ruggedness than with mean elevation. Overall, correlation values are also higher than those found for average local drought characteristics, and visual inspection of the spatial distribution (not shown here) does show a quite homogeneous distribution of drought characteristics change between the mountains (especially on the windward side, i.e. the one facing the Po plain) and the plains and hills. The only outliers are the Aosta valley in the nord-west and another valley close to the western border, with changes often in common with the lowlands.

Still, most of the changes found by comparing the two periods are not found to be significant according to the two sample t-test, and thus do not denote a change in the probability distribution of local drought characteristics. The cells with significant changes (reported in Figure 5) are mostly distributed between two areas: changes towards more severe (according to SPI-12, SPEI-3 and SPEI-12), longer (by both indices at the 3 month scale) and more intense (by both indices at the 12 month scale) droughts are reported for the eastern-most part of the domain; changes towards less severe and shorter droughts are reported mostly in the northern part of the alpine chain for SPI/SPEI at the 3 month scale, while almost no significant shifts towards less intense local droughts are reported.

4.3 Region-wide drought event analysis

This section shows the results obtained from the analysis of region wide drought events (see Section 4.3). Similarly to the previous sections, both the characteristics of drought events and their change over time are discussed.

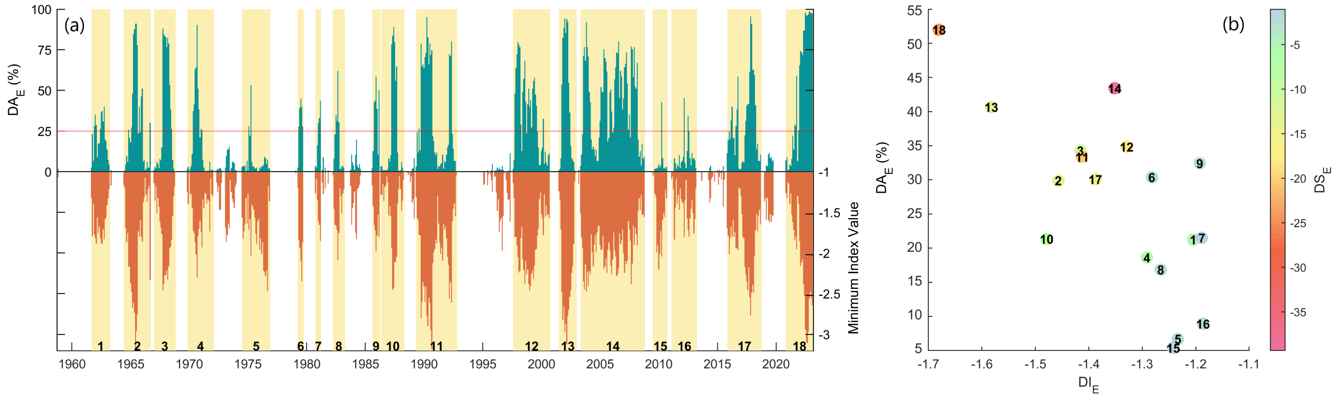

Figure 6. Region-wide drought event analysis conducted on SPEI-12. **(a)** Time series of percentage of cells in drought condition (only the portion below the -1 threshold, upper part of the diagram) and minimum index value in the domain (lower part of the diagram). Each event is highlighted in yellow and labeled. **(b)** Drought event characteristics: drought intensity (DI_E), mean drought area (DA_E) and drought severity (DS_E).

4.3.1 Drought event characteristics

Region-wide drought events are calculated from SPI and SPEI index series at 3 and 12 month scales. As the most interesting example, Figure 6 shows the result for SPEI-12. The analysis displays similar results between the two indices at the same time scale, with all main events identified by both SPI and SPEI, and high agreement between the extent of the area in drought conditions over time. The analysis at the 3-month scale reports about 60 events (see supplementary Figure A2), while the analysis at the 12-month scale (for SPEI-12 see Figure 6, for SPI-12 see supplementary Figure A3) reports less than 20 events. Region-wide drought events at the longer time scale are also far more severe and longer than those at the shorter time scale, but intensity and area values are similar. Regarding relative differences between the drought characteristics between SPI and SPEI at both time scales, $\overline{DS}_E$ is similar between the two indices, $\overline{DD}_E$ is higher for SPEI, and both $\overline{DI}_E$ and $\overline{DA}_E$ are higher for SPI. On the other hand, when considering the mean highest area affected by drought conditions in every single event both indices report similar results at both time scales. Overall, this indicates that the same deficit tends to affect a slightly wider area, with a higher intensity but for less time when only precipitation is considered, while it tends to affect the same overall area with less intensity and for a longer time when both precipitation and temperature are considered.

Region-wide drought event analysis on SPI-12 and SPEI-12 was also useful in indicating the main drought events that happened in the region in the last 60 years. Of these, the last one, starting in the winter of 2021 and still ongoing at the end of the available data timeseries, was identified as perhaps the most extreme in the series. In particular, the wide area affected by drought during this event and its severity, second only to the longest 2001-2008 event, mark it as an exceptional drought for the region. The intensity value is also the highest of all detected events, but this may not be significant given that this last

Table 3. Drought event characteristics before and after 1990. Values in italic font font denote significant differences between the two distributions at 5% significance.

	Number of events		$\overline{\mathbf{DS}}_{\mathbf{E}}$		$\overline{\mathbf{DD}}_{\mathbf{E}}$ **(months)**		$\overline{\mathbf{DI}}_{\mathbf{E}}$		$\overline{\mathbf{DA}}_{\mathbf{E}}$ **(%)**	
	Pre 1990	Post 1990	Pre 1990	Post 1990	Pre 1990	Post 1990	Pre 1990	Post 1990	Pre 1990	Post 1990
SPI-3	31	28	-3.24	-3.30	5.68	5.90	-1.45	-1.50	38.51	35.13
SPEI-3	27	32	-3.10	-3.40	6.18	6.56	-1.32	-1.36	37.50	32.05
SPI-12	12	5	*-7.14*	*-19.34*	*14.33*	*36.60*	-1.37	-1.42	31.61	32.05
SPEI-12	11	7	-6.92	-16.14	20.27	32.28	-1.31	-1.39	24.24	30.77

event had not yet ended at the time the analysis was done. Certainly, the fact that its severity is higher than the severity of the 2001-2002 event as detected through SPEI-12, also adds to how exceptional this last event is.

4.3.2 Temporal analysis of drought event characteristics

Trend analysis reports no significant results for the drought characteristics of region-wide drought events. Confronting the values before and after 1990 does show results consistent with those found for local droughts (Table 3): drought events have become more severe, longer and more intense at both time scales. Also similar to drought runs, the number of drought events has increased at the shorter 3-month time scale while it has decreased at the longer 12-month scale. Another difference is in the $\overline{DA}_E$, which has decreased at the 3-month time scale and has increased at the 12-month time scale. Overall, this seems to indicate that, on a region-wide level, drought conditions have worsened between the periods 1960-1990 and 1990-2020, with short-term deficits becoming more common over slightly smaller areas, leading to more generalised deficits over wider areas at the longer time scales. Despite many of the described changes not being significant according to the two-sample t-test, $\overline{DS}_E$ and $\overline{DD}_E$ for SPI-12 do report a statistically significant shift in the mean before and after 1990. Changes in $\overline{DS}_E$ and $\overline{DD}_E$ for SPEI-12 also report p-values close to the 5% level, although not falling below the 5% threshold. This seems to confirm that the shift towards worse region-wide drought conditions (higher severity and longer duration) is more evident at longer time scales, and that this shift is mainly caused by a change in precipitation patterns. Despite the apparent importance of precipitation, the only significant trend in terms of the percentage of the domain in drought conditions (index lower than -1) over time is found for SPEI-12, with a slope coefficient of 2.92×10^{-4}/year.

5 Discussion and conclusion

In this study, 60 years of precipitation and temperature data are analyzed in order to characterise changes in drought conditions in the Piedmont and Aosta Valley area. In Section 1 three questions were posed. The first question asked whether there are temporal trends in drought indices such as SPI and SPEI, and how do these trends translate into changes in the characteristics of drought events (in terms of duration, severity, and intensity). Evidence of widespread drying trends in the region is found through the trend analysis of SPI and SPEI series. Temperature plays a key role in defining these drying trends, as the SPEI reports negative trends for wider areas and with greater slope coefficients than SPI. This is to be expected given the clear trends in temperature due to climate change and is consistent with other studies conducted in the area (see e.g., Falzoi et al., 2019; Baronetti et al., 2020). When moving from drought indices to drought event identification, it is interesting to note that the start and end of single drought periods seem to be mainly determined by precipitation anomalies, in contrast to the importance of temperature in determining long-term conditions. Despite the worsening of drought conditions related to precipitation and temperature being clear, the effects on the characteristics of individual drought events are weaker. Some evidence of an increase in the severity, duration and intensity of drought periods after 1990 is found, although often not statistically significant. A tendency for drought periods at 3-month time scale to become more numerous, and for drought periods at 12-month time scale to become less numerous is observed, both at a local and regional scale. Thus, while the percentage of time under drought conditions has become greater at both time scales, it seems that a larger amount of short-term deficits aggregate into long-term deficits with higher duration. In addition to this, a significant positive trend in the percentage of the area under drought conditions according to SPEI-12 is detected. Overall, however, changes in local drought characteristics between the two halves of the analysed series are seldom significant, making it difficult to assess whether the increase in severity, duration and intensity of drought periods is actually part of a general tendency, that would be coherent with the detected worsening drought conditions.

The higher resolution of the analyzed data, compared to previous studies, makes it possible to show quite heterogeneous results regarding the presence of drying/wetting trends, as well as drought characteristics, in different portions of the region. As a possible explanation of this result, our analysis studies relations between terrain characteristics and drought characteristics, finding several significant correlations. This type of analysis is in common with a growing body of literature focused on the elevation effects on drought characteristics, with studies conducted in the Qinghai–Tibet plateau (Feng et al., 2020), the Lorestan province in Iran (Hosseini et al., 2020), the Indus river basin (Dubey et al., 2023) and the Canary Islands (Carrillo et al., 2023). These studies, using mean elevation as a topographic variable, find different results in regards to the distribution of drought trends at high/low elevations, and as such no general claim about the tendency of different elevation areas to show drying/wetting trends can be made. The second question in the introductory section asked whether there is a relationship between drought trends and topographical characteristics of the landscape and, if so, whether elevation is the topographical variable most correlated to these trends. Terrain characteristics and mean elevation show significant influence on the observed trends and changes in drought characteristics, with drying trends being more severe the lower and less rugged the area. In fact, when the mountainous parts and the flat part of the domain are considered separately, the first shows no significant drought trends, while the second reports significant drying trends for both SPI and SPEI at multiple timescales. This is particularly true for the flat areas of the region, where trends are stronger than in low elevated rugged (hilly) areas. In the case of drought period characteristics, decreases in their severity, duration and intensity are mostly found in the alpine range, while increases are mostly found in the smoother and low lying areas. Overall, drought characteristics and changes in time seem to be better correlated to the terrain ruggedness than to elevation alone. Thus, our finding of more severe drying trends and worsening drought characteristics in the lower altitude part of the region proves the importance of considering topographic effects in areas with highly diverse terrain. More importantly, our study shows that mean elevation, although certainly a variable to be considered, shouldn't be the only topographic variable taken into account.

The third question in the introductory section asked whether the outcomes depend on the chosen spatial scale of the analysis. Interestingly, the local drought analysis and the region-wide analysis result in some differences. Changes in the characteristics of local drought periods are affected by temperature increase, as drought periods obtained from SPEI series show more pronounced increases in severity, duration and intensity than those obtained from SPI series. Contrary to this, drought events at a region-wide scale show more marked shifts in severity and duration for SPI than for SPEI, denoting a more significant influence of regional precipitation patterns than of temperature on droughts at a regional scale. It would be of interest to understand if this is valid for the region of interest, north-western Italy, or if a similar result could be valid in other areas of the world, and, more generally, what could be the causes, from a meteorological and climatic point of view.

The same consideration can be done for the other results of our analyses. Although strong correlations between drought trends and the mean elevation and ruggedness of the terrain are found, the attribution of these results to physical phenomena is not straightforward. The presented methodology doesn't focus on this aspect and, given the complexity of the involved phenomena, attribution is outside the scope of our study. However, our finding of different meteorological conditions between the alpine chain and the surrounding Po plain is consistent with other studies concerning the presence of an increase in alpine summer convective precipitation not in common with the surrounding areas (Giorgi et al., 2016; Grose et al., 2019).

In this study we restrict our focus to near-past and current conditions and do not consider predictions of future conditions (although strong drying trends in some portions of the study area are detected). Further research is needed to study how the local and regional drought characteristics of areas at different elevations and with different reliefs may evolve under climate change. Still, the results presented in this paper can be useful not only for the Piedmont and Aosta Valley region, where they could be the input for analyses of soil moisture and hydrological droughts, but also for other areas and for drought research in general, showing the need to conduct drought studies at different spatio-temporal scales, showing the need to consider areas with distinct topographical features as well as giving an indication of which areas are more likely to face dryer conditions.

Data availability. The data that support the findings of this study are openly available in the NWIOI data set at *https://www.arpa.piemonte.it/rischinaturali/tematismi/clima/confronti-storici/dati/dati.html* maintained and updated by the Forecast Systems Department of the Regional Environmental Protection Agency of Piedmont (*Dipartimento Sistemi Previsionali - Arpa Piemonte*).

Appendix A: Supplementary figures

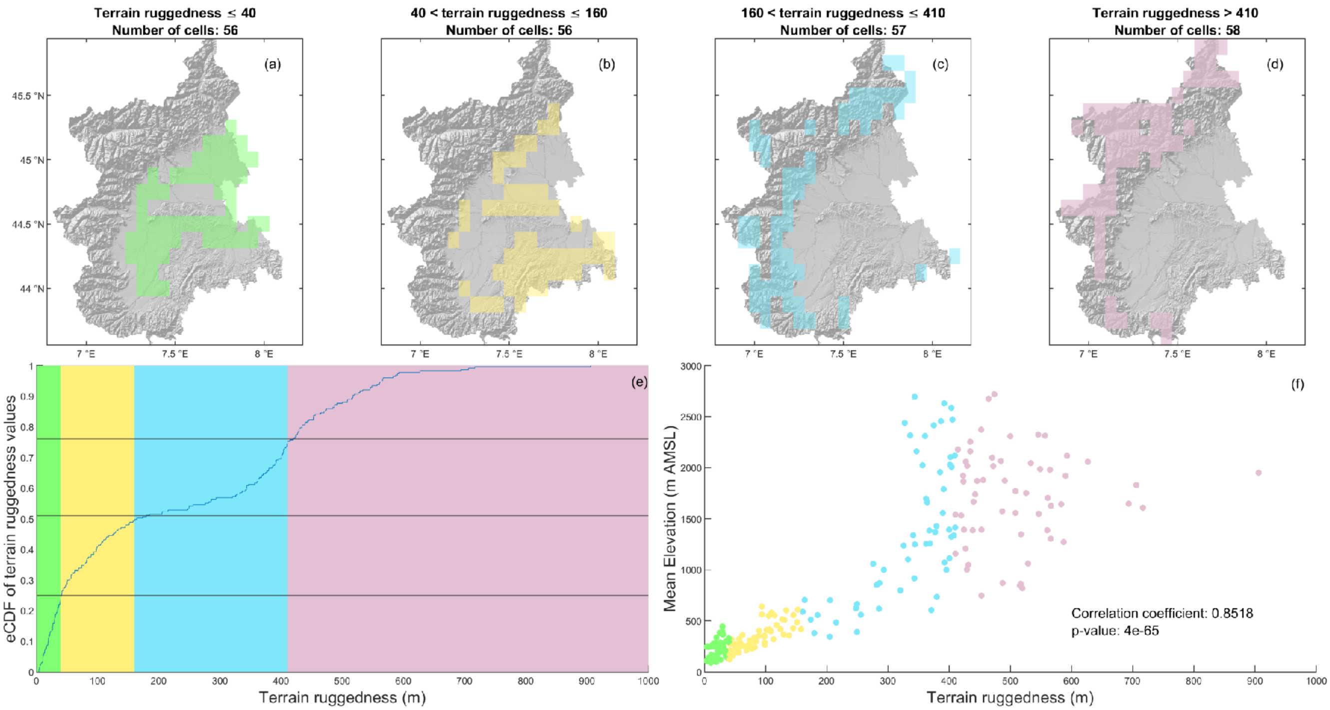

Figure A1. Areas classified using mean cell elevation and terrain ruggedness, calculated as the standard deviation of elevation values inside each cell. **(a-d)** Areas belonging to classes defined based on terrain ruggedness, corresponding to the A to D areas cited in Figure 3. **(e)** Empirical cumulative distribution function (eCDF) of the terrain ruggedness values. **(F)** Scatter plot between terrain ruggedness and mean elevation for each cell and relative Pearson correlation coefficient.

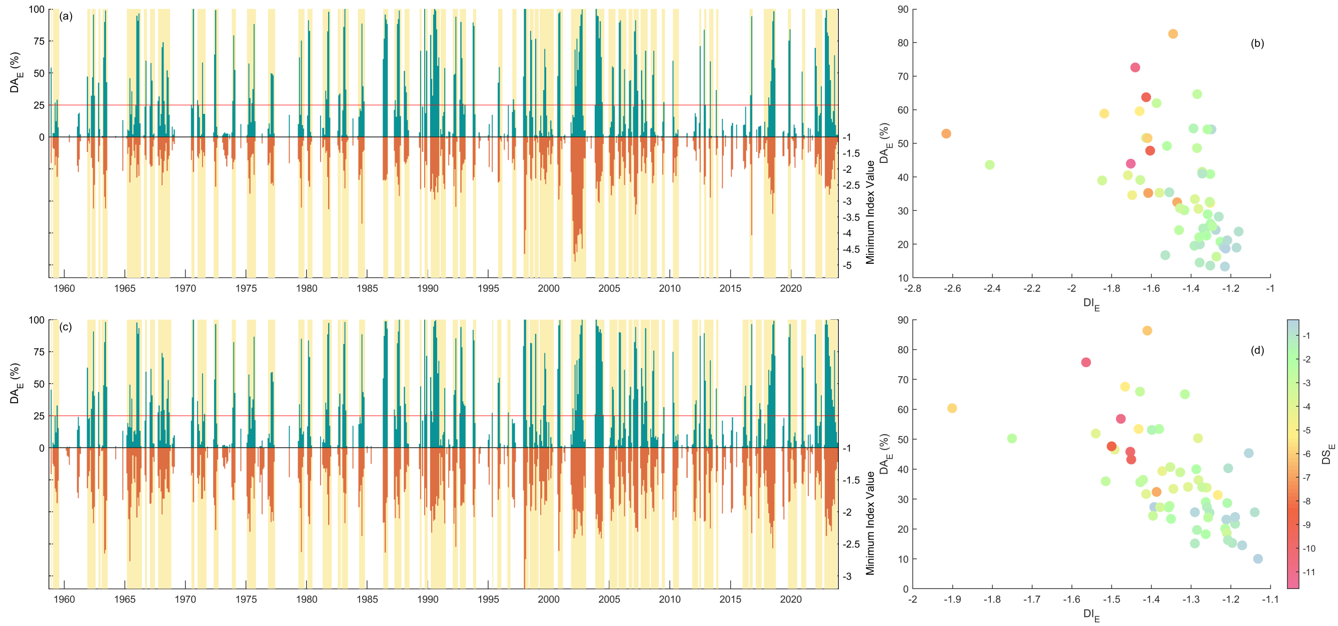

Figure A2. Region-wide drought event analysis conducted on the indices at 3 month scale. **(a)** Series of percentage of cells in drought condition (below the -1 threshold) and the minimum index value in the domain for SPI-3. **(b)** Drought event characteristics for SPI-3. **(c)** Series of percentage of cells in drought condition (below the -1 threshold) and the minimum index value in the domain for SPEI-3. **(d)** Drought event characteristics for SPEI-3.

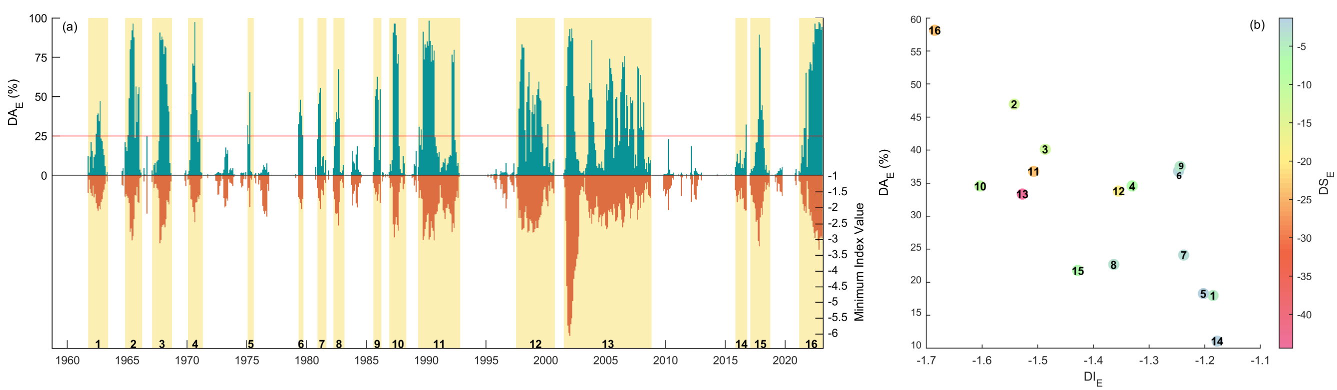

Figure A3. Region-wide drought event analysis conducted on SPI-12. **(a)** Series of percentage of cells in drought condition (below the -1 threshold) and the minimum index value in the domain. Each event is highlighted in yellow and labeled. **(b)** Drought event characteristics.

Author contributions. M.E., S.T., A.V. and R.R. contributed to the design of the research, to the analysis of the results and to the writing of the manuscript. M.E. carried out the analysis.

Competing interests. The authors declare no competing interests.

Acknowledgements. This study was carried out within the RETURN Extended Partnership and received funding from the European Union Next-GenerationEU (National Recovery and Resilience Plan – NRRP, Mission 4, Component 2, Investment 1.3 – D.D. 1243 2/8/2022, PE0000005).

References

Angelidis, P., Maris, F., Kotsovinos, N., and Hrissanthou, V.: Computation of Drought Index SPI with Alternative Distribution Functions, Water Resources Management, 26, 2453–2473, https://doi.org/10.1007/s11269-012-0026-0, number: 9, 2012.

Arpa Piemonte: Il Piemonte nel Cambiamento Climatico, http://www.arpa.piemonte.it/pubblicazioni-2/pubblicazioni-anno-2007/pdf-il-piemonte-nel-cambiamento-climatico, 2007.

Arpa Piemonte, D. R. N. e. A. e. D. S. P. and Regione Piemonte, Energia e Territorio Settore Progettazione Strategica e Green Economy, D. A.: Analisi degli scenari di clima regionale del periodo 2011- 2100, https://www.regione.piemonte.it/web/sites/default/files/media/documenti/2021-02/analisi_scenari_clima_regionale_periodo_2011-_2100.pdf, 2020.

Arpa Piemonte, Dipartimento Sistemi Provisionali: NWIOI Dataset, https://www.arpa.piemonte.it/rischinaturali/tematismi/clima/confronti-storici/dati/dati.html, last acces: 12 February 2024, 2011.

Ault, T. R.: On the essentials of drought in a changing climate, Science, 368, https://doi.org/10.1126/science.aaz549, 2020.

Baronetti, A., González-Hidalgo, J. C., Vicente-Serrano, S. M., Acquaotta, F., and Fratianni, S.: A weekly spatio-temporal distribution of drought events over the Po Plain (North Italy) in the last five decades, International Journal of Climatology, 40, 4463–4476, https://doi.org/10.1002/joc.6467, number: 10, 2020.

Baronetti, A., Dubreuil, V., Provenzale, A., and Fratianni, S.: Future droughts in northern Italy: high-resolution projections using EURO-CORDEX and MED-CORDEX ensembles, Climatic Change, 172, 22, https://doi.org/10.1007/s10584-022-03370-7, 2022.

Beguería, S., Vicente-Serrano, S. M., Reig, F., and Latorre, B.: Standardized precipitation evapotranspiration index (SPEI) revisited: parameter fitting, evapotranspiration models, tools, datasets and drought monitoring, International Journal of Climatology, 34, 3001–3023, https://doi.org/10.1002/joc.3887, number: 10, 2014.

Bordi, I. and Sutera, A.: An analysis of drought in Italy in the last fifty years, Il Nuovo Cimento C, 25, 2002.

Brian Ayugi, Emmanuel Olaoluwa Eresanya, A. O. O. F. K. O. E. C. O.-C. O. O. C. M. A. V. N. D. O. R. A. M. T. D. R. M. V. O.: Review of Meteorological Drought in Africa: Historical Trends, Impacts, Mitigation Measures, and Prospects, Pure and Applied Geophysics, 179, 1365–1386, https://doi.org/10.1007/s00024-022-02988-z, 2022.

Brunetti, M., Maugeri, M., Nanni, T., and Navarra, A.: Droughts and extreme events in regional daily Italian precipitation series, International Journal of Climatology, 22, 543–558, https://doi.org/10.1002/joc.751, number: 5, 2002.

Burek, P., Satoh, Y., Fischer, G. W., Kahil, M. T., Scherzer, A., Tramberend, S., Nava, L. F., Wada, Y., Eisner, S., Flörke, M., Hanasaki, N., Magnuszewski, P., Cosgrove, B., and Wiberg, D.: Water Futures and Solution - Fast Track Initiative (Final Report), 2016.

Caloiero, T., Caroletti, G. N., and Coscarelli, R.: IMERG-Based Meteorological Drought Analysis over Italy, Climate, 9, 65, https://doi.org/10.3390/cli9040065, number: 4, 2021.

Carrillo, J., Hernández-Barrera, S., Expósito, F. J., Díaz, J. P., González, A., and Pérez, J. C.: The uneven impact of climate change on drought with elevation in the Canary Islands, npj Climate and Atmospheric Science, 6, 31, https://doi.org/10.1038/s41612-023-00358-7, 2023.

Choi, S. C. and Wette, R.: Maximum Likelihood Estimation of the Parameters of the Gamma Distribution and Their Bias, Technometrics, 11, 683–690, https://doi.org/10.1080/00401706.1969.10490731, 1969.

Ciccarelli, N., Von Hardenberg, J., Provenzale, A., Ronchi, C., Vargiu, A., and Pelosini, R.: Climate variability in north-western Italy during the second half of the 20th century, Global and Planetary Change, 63, 185–195, https://doi.org/10.1016/j.gloplacha.2008.03.006, 2008.

Cohen, J.: A Coefficient of Agreement for Nominal Scales, Educational and Psychological Measurement, 20, 37–46, https://doi.org/10.1177/001316446002000104, 1960.

Collaud Coen, M., Andrews, E., Bigi, A., Martucci, G., Romanens, G., Vogt, F. P. A., and Vuilleumier, L.: Effects of the prewhitening method, the time granularity, and the time segmentation on the Mann–Kendall trend detection and the associated Sen's slope, Atmospheric Measurement Techniques, 13, 6945–6964, https://doi.org/10.5194/amt-13-6945-2020, 2020.

Crausbay, S. D., Betancourt, J., Bradford, J., Cartwright, J., Dennison, W. C., Dunham, J., Enquist, C. A., Frazier, A. G., Hall, K. R., Littell, J. S., Luce, C. H., Palmer, R., Ramirez, A. R., Rangwala, I., Thompson, L., Walsh, B. M., and Carter, S.: Unfamiliar Territory: Emerging Themes for Ecological Drought Research and Management, One Earth, 3, 337–353, https://doi.org/10.1016/j.oneear.2020.08.019, number: 3, 2020.

Dai, A.: Drought under global warming: a review, WIREs Climate Change, 2, 45–65, https://doi.org/10.1002/wcc.81, 2011.

Dai, A.: Increasing drought under global warming in observations and models, Nature Climate Change, 3, 52–58, https://doi.org/10.1038/nclimate1633, 2013.

Dubey, A., Swami, D., Gupta, V., and Joshi, N.: From the peaks to the plains: Investigating the role of elevation in governing drought dynamics over the Indus river basin, Atmospheric Research, 291, 106 824, https://doi.org/10.1016/j.atmosres.2023.106824, 2023.

Falzoi, S., Acquaotta, F., Pulina, M. A., and Fratianni, S.: Hydrological drought analysis in Continental Temperate and Mediterranean environment during the period 1981-2017, Italian Journal of Agrometeorology, pp. 13–23 Pages, https://doi.org/10.13128/IJAM-798, artwork Size: 13-23 Pages Publisher: Italian Journal of Agrometeorology, 2019.

Feng, W., Lu, H., Yao, T., and Yu, Q.: Drought characteristics and its elevation dependence in the Qinghai–Tibet plateau during the last half-century, Scientific Reports, 10, 14 323, https://doi.org/10.1038/s41598-020-71295-1, 2020.

García-León, D., Standardi, G., and Staccione, A.: An integrated approach for the estimation of agricultural drought costs, Land Use Policy, 100, 104 923, https://doi.org/10.1016/j.landusepol.2020.104923, 2021.

Giorgi, F., Torma, C., Coppola, E., Ban, N., Schär, C., and Somot, S.: Enhanced summer convective rainfall at Alpine high elevations in response to climate warming, Nature Geoscience, 9, 584–589, https://doi.org/10.1038/ngeo2761, 2016.

González-Hidalgo, J. C., Vicente-Serrano, S. M., Peña-Angulo, D., Salinas, C., Tomas-Burguera, M., and Beguería, S.: High-resolution spatio-temporal analyses of drought episodes in the western Mediterranean basin (Spanish mainland, Iberian Peninsula), Acta Geophysica, 66, 381–392, https://doi.org/10.1007/s11600-018-0138-x, 2018.

Greene, C. A., Thirumalai, K., Kearney, K. A., Delgado, J. M., Schwanghart, W., Wolfenbarger, N. S., Thyng, K. M., Gwyther, D. E., Gardner, A. S., and Blankenship, D. D.: The Climate Data Toolbox for MATLAB, Geochemistry, Geophysics, Geosystems, 20, 3774–3781, https://doi.org/10.1029/2019GC008392, 2019.

Grose, M. R., Syktus, J., Thatcher, M., Evans, J. P., Ji, F., Rafter, T., and Remenyi, T.: The role of topography on projected rainfall change in mid-latitude mountain regions, Climate Dynamics, 53, 3675–3690, https://doi.org/10.1007/s00382-019-04736-x, 2019.

Habib, M.: Evaluation of DEM interpolation techniques for characterizing terrain roughness, CATENA, 198, 105 072, https://doi.org/10.1016/j.catena.2020.105072, 2021.

Hanel, M., Rakovec, O., Markonis, Y., Máca, P., Samaniego, L., Kyselý, J., and Kumar, R.: Revisiting the recent European droughts from a long-term perspective, Scientific Reports, 8, 9499, https://doi.org/10.1038/s41598-018-27464-4, number: 1, 2018.

Hargreaves, G. H. and Samani, Z. A.: Reference Crop Evapotranspiration from Temperature, Applied Engineering in Agriculture, 1, 96–99, https://doi.org/10.13031/2013.26773, 1985.

Haslinger, K. and Blöschl, G.: Space-Time Patterns of Meteorological Drought Events in the European Greater Alpine Region Over the Past 210 Years: SPACE-TIME PATTERNS OF DROUGHT EVENTS, Water Resources Research, 53, 9807–9823, https://doi.org/10.1002/2017WR020797, number: 11, 2017.

Haslinger, K., Chimani, B., and Böhm, R.: 200 years of liquid and solid precipitation in major river systems originating in the Greater Alpine Region, pp. 1798–, 2012.

Hayes, M., Svoboda, M., Wilhite, D., and Vanyarkho, O.: Monitoring the 1996 Drought Using the Standardized Precipitation Index, Bulletin of The American Meteorological Society - BULL AMER METEOROL SOC, 80, 429–438, https://doi.org/10.1175/1520-0477(1999)080<0429:MTDUTS>2.0.CO;2, 1999.

Hoerling, M., Eischeid, J., Perlwitz, J., Quan, X., Zhang, T., and Pegion, P.: On the Increased Frequency of Mediterranean Drought, Journal of Climate, 25, 2146–2161, https://doi.org/10.1175/JCLI-D-11-00296.1, number: 6, 2012.

Hosking, J. R. M.: The theory of probability weighted moments, 1986.

Hosseini, T. S. M., Hosseini, S. A., Ghermezcheshmeh, B., and Sharafati, A.: Drought hazard depending on elevation and precipitation in Lorestan, Iran, Theoretical and Applied Climatology, 142, 1369–1377, https://doi.org/10.1007/s00704-020-03386-y, 2020.

IDMP: Drought and Water Scarcity, no. 1284 in WMO, Global Water Partnership, Stockholm, Sweden, 2022.

Karagulle, D., Frye, C., Sayre, R., Breyer, S., Aniello, P., Vaughan, R., and Wright, D.: Modeling global Hammond landform regions from 250-m elevation data, Transactions in GIS, 21, 1040–1060, https://doi.org/10.1111/tgis.12265, 2017.

Kulkarni, A. and Storch, H. v.: Monte Carlo experiments on the effect of serial correlation on the Mann-Kendall test of trend, volume: 4, 1995.

Laimighofer, J. and Laaha, G.: How standard are standardized drought indices? Uncertainty components for the SPI & SPEI case, Journal of Hydrology, 613, 128 385, https://doi.org/10.1016/j.jhydrol.2022.128385, 2022.

Mann, H. B.: Nonparametric tests against trend, Econometrica, 13, 245—-259, https://doi.org/10.2307/1907187, 1945.

McKee, T. B., Doesken, N. J., and Kleist, J. R.: THE RELATIONSHIP OF DROUGHT FREQUENCY AND DURATION TO TIME SCALES, 1993.

Mountain Research Initiative EDW Working Group: Elevation-dependent warming in mountain regions of the world, Nature Climate Change, 5, 424–430, https://doi.org/10.1038/nclimate2563, 2015.

Palazzi, E., Mortarini, L., Terzago, S., and Von Hardenberg, J.: Elevation-dependent warming in global climate model simulations at high spatial resolution, Climate Dynamics, 52, 2685–2702, https://doi.org/10.1007/s00382-018-4287-z, 2019.

Pavan, V., Antolini, G., Barbiero, R., Berni, N., Brunier, F., Cacciamani, C., Cagnati, A., Cazzuli, O., Cicogna, A., De Luigi, C., Di Carlo, E., Francioni, M., Maraldo, L., Marigo, G., Micheletti, S., Onorato, L., Panettieri, E., Pellegrini, U., Pelosini, R., Piccinini, D., Ratto, S., Ronchi, C., Rusca, L., Sofia, S., Stelluti, M., Tomozeiu, R., and Torrigiani Malaspina, T.: High resolution climate precipitation analysis for north-central Italy, 1961–2015, Climate Dynamics, 52, 3435–3453, https://doi.org/10.1007/s00382-018-4337-6, number: 5-6, 2019.

Pepin, N. C., Arnone, E., Gobiet, A., Haslinger, K., Kotlarski, S., Notarnicola, C., Palazzi, E., Seibert, P., Serafin, S., Schöner, W., Terzago, S., Thornton, J. M., Vuille, M., and Adler, C.: Climate Changes and Their Elevational Patterns in the Mountains of the World, Reviews of Geophysics, 60, https://doi.org/10.1029/2020RG000730, 2022.

Perosino, G. C. and Zaccara, P.: Elementi climatici del Piemonte, http://www.crestsnc.it/divulgazione/media/clima-piemonte.pdf, 2006.

Pörtner, H.-O., Roberts, D., Tignor, M., Poloczanska, E., Mintenbeck, K., Alegría, A., Craig, M., Langsdorf, S., Löschke, S., Möller, V., Okem, A., Rama, B., Belling, D., Dieck, W., Götze, S., Kersher, T., Mangele, P., Maus, B., Mühle, A., and Weyer, N.: Climate Change 2022: Impacts, Adaptation and Vulnerability Working Group II Contribution to the Sixth Assessment Report of the Intergovernmental Panel on Climate Change, https://doi.org/10.1017/9781009325844., 2022.

Rangwala, I. and Miller, J. R.: Climate change in mountains: a review of elevation-dependent warming and its possible causes, Climatic Change, 114, 527–547, https://doi.org/10.1007/s10584-012-0419-3, 2012.

Rasch, D., Kubinger, K. D., and Moder, K.: The two-sample t test: pre-testing its assumptions does not pay off, Statistical Papers, 52, 219–231, https://doi.org/10.1007/s00362-009-0224-x, 2011.

Robinson, N., Regetz, J., and Guralnick, R. P.: EarthEnv-DEM90: A nearly-global, void-free, multi-scale smoothed, 90m digital elevation model from fused ASTER and SRTM data, ISPRS Journal of Photogrammetry and Remote Sensing, 87, 57–67, https://doi.org/10.1016/j.isprsjprs.2013.11.002, 2014.

Sayre, R., Frye, C., Karagulle, D., Krauer, J., Breyer, S., Aniello, P., Wright, D. J., Payne, D., Adler, C., Warner, H., VanSistine, D. P., and Cress, J.: A New High-Resolution Map of World Mountains and an Online Tool for Visualizing and Comparing Characterizations of Global Mountain Distributions, Mountain Research and Development, 38, 240–249, https://doi.org/10.1659/MRD-JOURNAL-D-17-00107.1, 2018.

Sen, P. K.: Estimates of the Regression Coefficient Based on Kendall's Tau, Journal of the American Statistical Association, 63, 1379–1389, https://doi.org/10.2307/2285891, 1968.

Sergio M. Vicente-Serrano, Dhais Peña-Angulo, S. B. F. D.-C. M. T.-B. I. N. L. G.-S. A. E. K.: Global drought trends and future projections, Phylosophical Transactions of the Royal Society A, 380, 20210 285, https://doi.org/10.1098/rsta.2021.0285, 2022.

Shevlyakov, G. L. and Oja, H.: Robust correlation: theory and applications, Wiley series in probability and statistics, Wiley, Chichester, West Sussex, United Kingdom, 2016.

Theil, H.: A rank-invariant method of linear and polynomial regression analysis. Part 1, Proceedings of the Koninklijke Nederlandse Akademie van Wetenschappen, 53, 386–392, 1950.

Tigkas, D., Vangelis, H., and Tsakiris, G.: DrinC: a software for drought analysis based on drought indices, Earth Science Informatics, 8, 697–709, https://doi.org/10.1007/s12145-014-0178-y, number: 3, 2015.

Trenberth, K. E., Dai, A., Van Der Schrier, G., Jones, P. D., Barichivich, J., Briffa, K. R., and Sheffield, J.: Global warming and changes in drought, Nature Climate Change, 4, 17–22, https://doi.org/10.1038/nclimate2067, 2014.

Turco, M., Zollo, A. L., Ronchi, C., De Luigi, C., and Mercogliano, P.: Assessing gridded observations for daily precipitation extremes in the Alps with a focus on northwest Italy, Natural Hazards and Earth System Sciences, 13, 1457–1468, https://doi.org/10.5194/nhess-13-1457-2013, 2013.

Uboldi, F., Lussana, C., and Salvati, M.: Three-dimensional spatial interpolation of surface meteorological observations from high-resolution local networks, Meteorological Applications, 15, 331–345, https://doi.org/10.1002/met.76, 2008.

Unesco, ed.: Nature-based solutions for water, no. 2018 in The United Nations world water development report, UNESCO, Paris, 2018.

Vicente-Serrano, S. M., Beguería, S., and López-Moreno, J. I.: A Multiscalar Drought Index Sensitive to Global Warming: The Standardized Precipitation Evapotranspiration Index, Journal of Climate, 23, 1696–1718, https://doi.org/10.1175/2009JCLI2909.1, number: 7, 2010.

Vogel, J., Paton, E., Aich, V., and Bronstert, A.: Increasing compound warm spells and droughts in the Mediterranean Basin, Weather and Climate Extremes, 32, 100 312, https://doi.org/10.1016/j.wace.2021.100312, 2021.

Wada, Y., Flörke, M., Hanasaki, N., Eisner, S., Fischer, G., Tramberend, S., Satoh, Y., Van Vliet, M. T. H., Yillia, P., Ringler, C., Burek, P., and Wiberg, D.: Modeling global water use for the 21st century: the Water Futures and Solutions (WFaS) initiative and its approaches, Geoscientific Model Development, 9, 175–222, https://doi.org/10.5194/gmd-9-175-2016, 2016.

Wallemacq, P., Guha-Sapir, D., McClean, D., CRED, and UNISDR: The Human Cost of Natural Disasters - A global perspective, 2015.

Wang, W., Chen, Y., Becker, S., and Liu, B.: Variance Correction Prewhitening Method for Trend Detection in Autocorrelated Data, Journal of Hydrologic Engineering, 20, 04015 033, https://doi.org/10.1061/(ASCE)HE.1943-5584.0001234, 2015.

Ward, P. J., Blauhut, V., Bloemendaal, N., Daniell, J. E., De Ruiter, M. C., Duncan, M. J., Emberson, R., Jenkins, S. F., Kirschbaum, D., Kunz, M., Mohr, S., Muis, S., Riddell, G. A., Schäfer, A., Stanley, T., Veldkamp, T. I. E., and Winsemius, H. C.: Review article: Natural hazard risk assessments at the global scale, Natural Hazards and Earth System Sciences, 20, 1069–1096, https://doi.org/10.5194/nhess-20-1069-2020, 2020.

Welch, B. L.: The Generalization of ‘Student’s’ Problem when Several Different Population Variances are Involved, Biometrika, 34, 28, https://doi.org/10.2307/2332510, 1947.

Whitehouse, D. J.: Handbook of surface metrology, Institute of Physics Publishing, Bristol, 1994.

World Meteorological Organization: Standardized precipitation index user guide., no. 1090 in WMO, Geneva, Switzerland, oCLC: 874098624, 2012.

Yevjevich, V. M.: Objective approach to definitions and investigations of continental hydrologic droughts, An, PhD Thesis, Colorado State University. Libraries, 1967.

Yue, S., Pilon, P., Phinney, B., and Cavadias, G.: The influence of autocorrelation on the ability to detect trend in hydrological series, Hydrological Processes, 16, 1807–1829, https://doi.org/10.1002/hyp.1095, 2002.